Journal of Institute of Science and Technology, 29(2), 117-128 (2024)
ISSN: 2467-9062 (print), e-ISSN: 2467-9240
https://doi.org/10.3126/jist.v29i2.70127

Research Article

CONFORMATIONAL ANALYSIS WITH ELUCIDATION ON MOLECULAR STRUCTURE, ELECTRONIC PROPERTIES, AND REACTIVITY OF THE NITROGLYCERIN FROM DFT

Tirth Raj Paneru[1,4] , Poonam Tandon[2], Bhawani Datt Joshi[3]*
[1]Central Department of General Science, Far Western University, Kanchanpur, 10400, Nepal
[2]Department of Physics, University of Lucknow, Lucknow, 226007, India
[3]Department of Physics, Siddhanath Science Campus, Tribhuvan University, Mahendranagar, 10406, Nepal
[4]Central Department of Physics, Tribhuvan University, Kirtipur, Kathmandu, Nepal
**Correspondence: bhawani.joshi@snsc.tu.edu.np, pbdjoshi@gmail.com*

(Received:** September 25, 2024; **Final Revision:** December 22, 2024**; Accepted:** December 23, 2024**)

ABSTRACT

This work involved the use of a one-dimensional potential energy surface scan to investigate the most stable conformer of nitroglycerin through conformational analysis. The goal of this work is to perform a quantum chemical calculation using density functional theory to gain insight onto molecular structure, reactivity, and electronic properties with the most stable structure. The most stable conformer of nitroglycerin was investigated, and its geometrical parameters were compared with experimental values. Non-covalent interaction was also performed, which illustrates the various intra-molecular interactions. The reactive sites were predicted using electrostatic potential surface analysis, with H16 as the best electrophile and N11 as a nucleophile, indicating the location of intermolecular interaction for biological action and crystal packing. The energy gap in the solvent ethanol was determined to be 6.628 eV, while in the gaseous medium; it was 6.684 eV, indicating that nitroglycerin is more reactive and polarizable in the solvent ethanol. A blue shift in the absorption wavelength of UV-Vis spectra was observed by employing time dependent density functional theory with a polarized continuum model in solvent ethanol. The hyperconjugative interactions π(O4-N10)$\rightarrow\sigma^*$(O5-N10), σ(O5-N10)$\rightarrow\pi^*$(O4-N10), LP(3)O8$\rightarrow\sigma^*$(O6-N11), and LP(3)O9$\rightarrow\pi^*$(O7-N12) have higher stabilization energy and are crucial to stabilizing the molecule.

Keywords: DOS spectrum, electrostatic potential, nitroglycerin, thermodynamic, UV-Vis spectra

INTRODUCTION

Nitroglycerin (NG), also known as trinitroglycerin, 1,2,3-trinitroxypropane, and glyceryl trinitrate, was discovered in 1847 by Ascanio Sobreo (Chen *et al.*, 2002; Marsh & Marsh, 2000). It is a colorless, heat and shock-sensitive explosive liquid that is denser than water and is used to make explosives like dynamite (Meenakshi *et al.*, 2012). Nitroglycerin serves as the primary energetic plasticizer in the nitrate ester-plasticized polyether (NEPE) propellant (Pei *et al.*, 2017; Yan *et al.*, 2013). Nitroglycerin is also prescribed in the initial treatment for angina pectoris and chronic heart failure (Sidhu *et al.*, 2015). It works by facilitating nitric oxide, which dilates blood vessels and increases the flow of blood to the myocardium (Ferreira & Mochly, 2012). Furthermore, intra-operative hypotension is induced with NG in 5% dextrose injection (Moazemi *et al.*, 2003). The vibrational spectra and thermodynamic properties of organic nitrates treated with HF, MP2, and B3LYP levels using the B3LYP method and the 6-31G (d,p) basis set were found to be in satisfactory agreement with the experimental results (Gong & Xiao, 2001). Yan *et al.* conducted the unimolecular breakdown of nitroglycerin in the gas phase; the findings indicate that the O−NO2 cleavage pathway proceeds more readily (Yan *et al.*, 2013). Meenakshi *et al.* performed theoretical computations at the B3PW91/6-31G(d,p) level of theory, and they compared the theoretical and experimental spectra of NG (Meenakshi *et al.*, 2012). The literature revealed that although the molecular and vibrational properties of nitroglycerin operated with DFT for small basis sets, for more exact calculations, larger basis sets with polarization and diffusion functions were not conducted far. The goal of our work is to perform a conformational analysis on NG to determine the most stable conformer and then treat molecular properties using the most stable conformer. Our research primarily focused on conformational stability, including the prediction of electronic transitions, reactive sites, non-covalent interactions, and thermodynamic properties of NG. For this work, we used density functional theory (DFT) and the B3LYP hybrid functional with basis set 6-311++G(d,p) to perform quantum chemical calculations. The most stable conformer of NG was achieved through one-dimensional potential energy scanning. The reduced density gradient (RDG) scatter plot revealed non-covalent interactions on the molecule. The electrostatic potential surface analysis predicts the electrophilic and nucleophilic sites in the molecule. The transition of electrons from donor to acceptor of the molecule is illustrated by UV-Vis absorption spectra. The natural bond orbital theory is also used for the better understanding of charge transfer in conjugative interactions within the molecule. Furthermore, thermodynamical analysis is used to know how thermodynamical parameters change with temperature.

MATERIALS AND METHODOLOGY

Computational details

The title molecule was subjected to quantum chemical calculations and geometry optimization using DFT in

the Gaussian 16 software package (M. J. Frisch *et al.*, 2009; Hohenberg & Kohn, 1964). Calculations were performed using the hybrid functional B3LYP and the polarization and diffusion basis set 6-311++G(d,p) (Becke, 1993; Dunning, 1989). The optimized structure and most significant transitions in the highest occupied molecular orbital (HOMO) and lowest unoccupied molecular orbital (LUMO) were visualized and plotted using GaussView 06 (Dennington *et al., 2016).* The mapping of the ESP onto the molecular van der Waals surface was conducted using Multiwfn 8 and VMD 1.9.4 (Humphrey *et al.*, 1996; Lu & Chen, 2012). The UV-Vis absorption spectra of NG, in gaseous and solvent phases, were studied by using TD-DFT at the B3LYP/6-311++G(d,p) level of theory (Cossi *et al.*, 2002; Stratmann *et al.*, 1998). GaussSum 3.0 software was used to construct the density of states (DOS) spectrum, with a full width at half maximum (FWHM) of 0.3 eV (O'Boyle *et al.*, 2008). The NBO 3.1 program, a part of the Gaussian 16 software, was used to perform natural orbital analysis (Glendening *et al.*, 1996).

RESULTS AND DISCUSSION

Conformational analysis

Nitroglycerin was obtained from the PubChem database and optimized in the Gaussian 16 software package with DFT and B3LYP/6-311++G(d,p) level theory. The optimized and chemical structures of NG are shown in Fig. 1. (a) and (b), respectively. To obtain the most stable conformer of NG, a one-dimensional potential energy scan was performed across flexible bonds N12-O3, O3-C15, C15-C13, C13-O1, C13-C14, O1-N10, C14-O2, and O2-N11 at corresponding dihedral angles ϕ1, ϕ2, ϕ2, ϕ4, ϕ5, ϕ6, ϕ7, and ϕ8, as represented by an arrow in Fig. 1 (a). The scan graph in Fig. 2 shows the relative energy fluctuation concerning the minimum energy as a change in dihedral angle at 10° in each step. The molecule was further optimized at both the global and local minima of the scan graph, resulting in a total of ten conformers of NG. All conformers with energy differences relative to the minimum energy conformer and their respective ground state energy are presented in Table 1. Five conformers with the energy differences of less than 0.56 kcal/mol are stable at room temperature, as depicted in Fig. 3 (Chaudhary *et al.*, 2020). Conformer I was the most stable conformer of nitroglycerin, with a ground state energy of −958.4669 a.u., which was less than −957.8146 a.u. when evaluated at the B3PW91/6-31G(d,p) level of theory (Meenakshi *et al.*, 2012). Conformer I was further optimized at the WB97XD/6-311++G(d,p) level of theory, and ground state energy was found to be –958.1515 a.u. This observation leads to the conclusion that NG operated with the B3LYP/6-311++G(d,p) level of theory, which gives more accurate ground state energy; hence, further work is performed with the same level of theory for the most stable conformer.

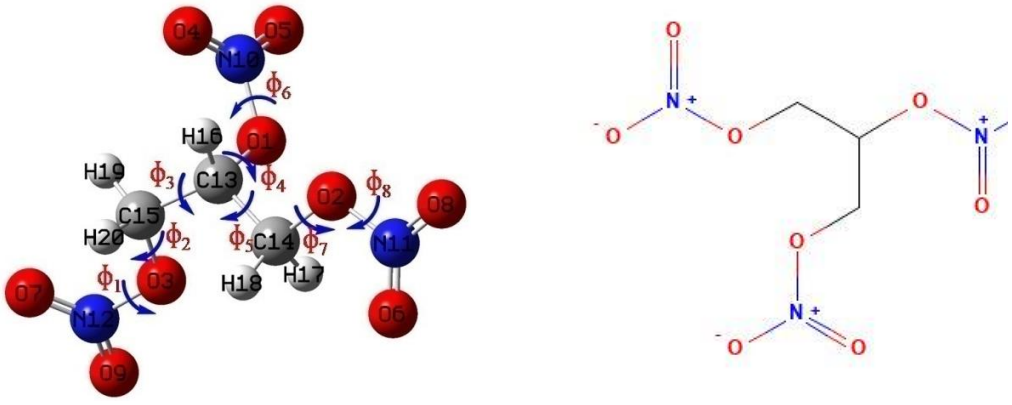

(a) **(b)**

Fig.1. (a) The optimized structure of nitroglycerin with numbering scheme showing arrow at the dihedral angle and (b) Chemical structure of nitroglycerin.

Optimized structure parameters

The conformer I has lower ground state energy than another conformer, making it the most stable. Its structural parameters, such as bond lengths and bond angles, were compared with experimental values found in the literature**.** The structural parameters (bond lengths, bond angles) for conformer I of NG calculated at the B3LYP/6-311++G(d,p) level of theory and their corresponding experimental values are presented in Table 2 (Antipin *et al.*, 1984). The bond lengths C14-H17, C13-H16, C14-H18, C15-H19, and C15-H20 showed a significant difference of 0.13, 0.14, 0.22, 0.15, and 0.13 Å, respectively, while the remaining bond lengths were in good agreement with the experimental values. The bond angles of O2-C14-C13, O2-C14-H17, O3-C15-C13, O3-C15-H19, and H19-C15-H20 differ from experimental values by 7.1, 7.7, 6.4, 7.6, and 5.0°, respectively, while the others are in good agreement. This difference is caused by intermolecular hydrogen bonding between hydrogen and oxygen in the crystal packing of nitroglycerin, but our calculation was performed for a single molecule in the gaseous state.

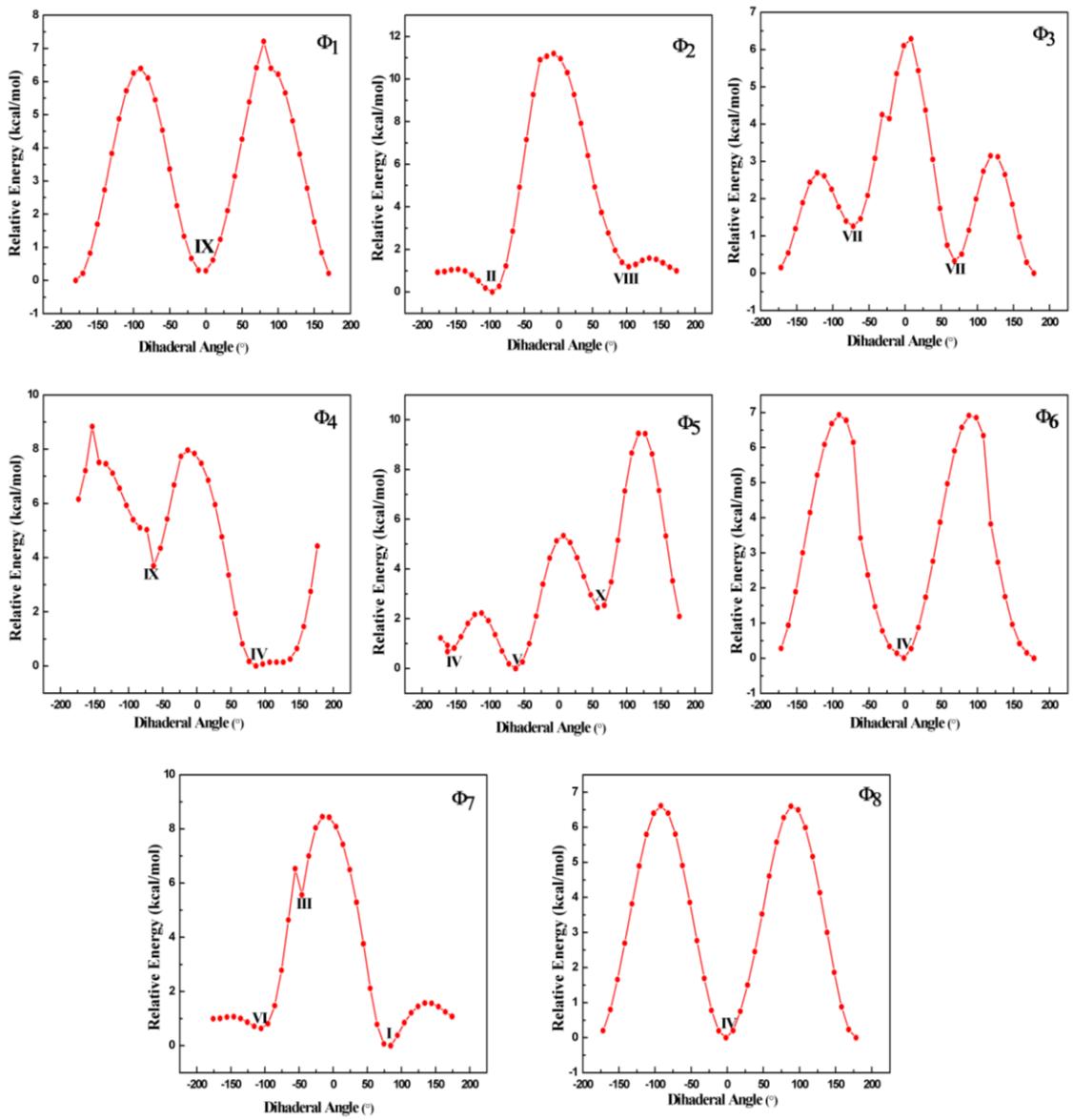

Figure 2. The Scan graph showing the variation of relative energy with the dihedral angle.

Table 1. Ten conformers of nitroglycerin with energy difference with respect to minimum energy structure along with their ground state energy.

Conformer	Dihaderal Angle (˚)	Energy (Hatree)	Energy (Kcal/mol)	Energy difference* (Kcal/mol)
I	Φ_7(C13-C14-O2-N11)	–958.4669	–601447.066	0
II	Φ_2(N12-O3-C15-C13)	–958.4666	–601446.906	0.161
III	Φ_7(C13-C14-O2-N11)	–958.4665	–601446.813	0.253
IV	Φ_4(C15-C13-O1-N10)	–958.4663	–601446.707	0.359
V	Φ_5(C15-C13-C14-O2)	–958.4662	–601446.632	0.434
VI	Φ_7(C13-C14-O2-N11)	–958.4657	–601446.305	0.761
VII	Φ_3(O3-C15-O13-O1)	–958.4652	–601446.005	1.062
VIII	Φ_1(O9-N12-O3-N15)	–958.4646	–601445.648	1.419
IX	Φ_5(C15-C13-C14-O2)	–958.4632	–601444.764	2.302
X	Φ_4(C15-C13-O1-N10)	–958.4587	–601441.913	5.153

*Relative energies of ten conformers with reference to minimum energy conformer I

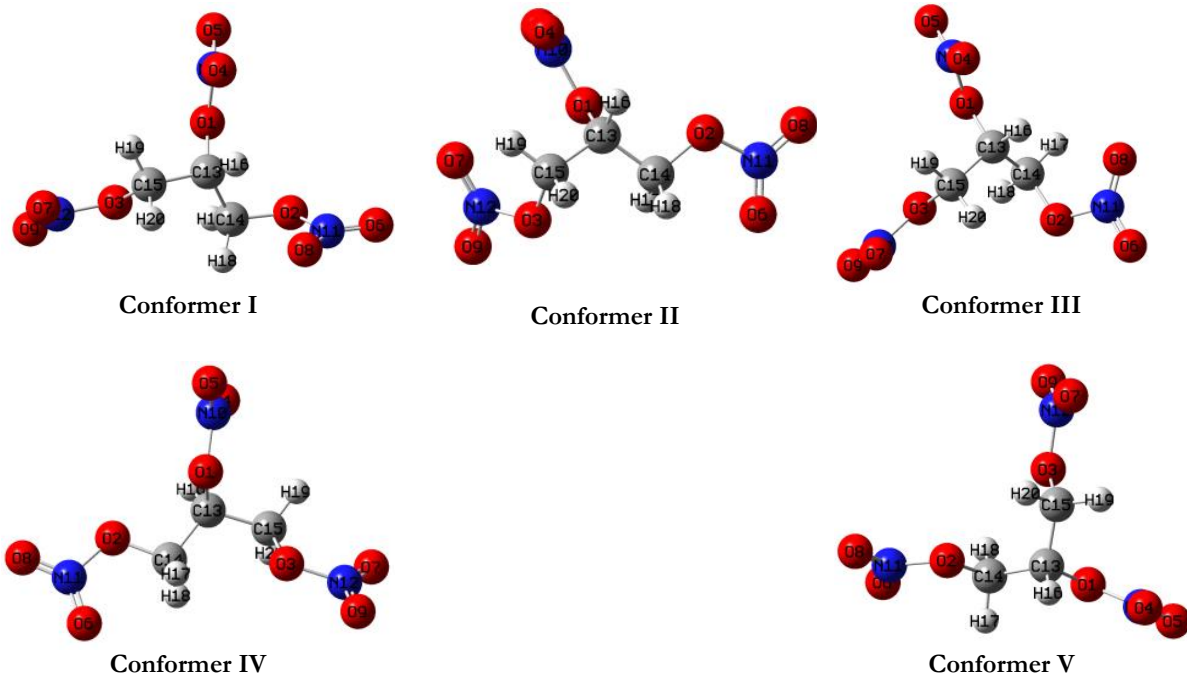

Figure 3. The optimized structure of the five stable conformer of nitroglycerin.

Table 2. The optimized structural parameters of nitroglycerin calculated at the B3LYP/6-311++G(d,p) level of theory with their corresponding experimental values.

Bond Name	Bond length (Å)	Experimental[a]	Angle Name	Angle (°)	Experimental[a]
R(O1-N10)	1.440	1.414	A(N10-O1-C13)	115.5	114.5
R(O1-C13)	1.445	1.458	A(O1-N10-O4)	117.4	118.5
R(O2-N11)	1.437	1.408	A(O1-N10-O5)	112.1	111.9
R(O2-C14)	1.437	1.453	A(O1-C13-C14)	105.1	104.2
R(O3-N12)	1.435	1.402	A(O1-C13-C15)	111.7	110.9
R(O3-C15)	1.442	1.445	A(O1-C13-H16)	109.3	110.0
R(O4-N10)	1.207	1.198	A(N11-O2-C14)	114.6	113.3
R(O5-N10)	1.193	1.204	A(O2-N11-O6)	112.4	112.1
R(O6-N11)	1.193	1.199	A(O2-N11-O8)	117.3	118.1
R(O7-N12)	1.205	1.202	A(O2-C14-C13)	112.3	105.2
R(O8-N11)	1.209	1.200	A(O2-C14-H17)	103.3	111.0
R(O9-N12)	1.195	1.199	A(O2-C14-H18)	110.4	111.0
R(C13-C14)	1.528	1.514	A(N12-O3-C15)	114.1	113.9
R(C13-C15)	1.524	1.512	A(O3-N12-O7)	116.9	118.5
R(C13-H16)	1.090	0.950	A(O3-N12-O9)	112.4	111.8
R(C14-H17)	1.089	0.960	A(O3-C15-C13)	106.5	112.9
R(C14-H18)	1.090	0.870	A(O3-C15-H19)	110.6	103.0
R(C15-H19)	1.090	0.940	A(O3-C15-H20)	110.1	110.0
R(C15-H20)	1.093	0.960	A(O4-N10-O5)	130.5	129.6
			A(O6-N11-O8)	130.3	129.8
			A(O7-N12-O9)	130.7	129.7
			A(C14-C13-C15)	113.1	112.3
			A(C14-C13-H16)	110.4	110.0

A(C13-C14-H17)	110.8	110.0
A(C13-C14-H18)	110.4	111.0
A(C15-C13-H16)	107.3	109.0
A(C13-C15-H19)	110.8	110.0
A(C13-C15-H20)	109.9	109.0
A(H17-C14-H18)	109.4	111.0
A(H19-C15-H20)	109.0	104.0

[a]Ref(Antipin *et al.*, 1984)

Non covalent interaction

Non-covalent interactions in the molecule were studied with the help of a reduced density gradient plot (Johnson *et al.*, 2010). The RDG scatter plot and isosurface plot were plotted with the help of Multiwfn and VMD software. The graph between RDG and signλ2(ϱ) shows three different types of interactions: van der Waals interactions, steric repulsions, and hydrogen bonds, represented by green, red, and blue color spikes (Paneru *et al.*, 2024). The type of interaction is determined by the sign of signλ2(ϱ), with repulsive interactions for signλ2(ϱ) > 0, attractive interactions for signλ2(ϱ) < 0, and Van der Waals weak interactions for signλ2(ϱ) = 0 (Jia *et al.*, 2019). The scatter graph for RDG and non-covalent interactions in NG is depicted in the isosurface plot shown in Fig. 4 (a) and (b), respectively. When the RDG graph and isosurface for NG were observed, no blue spikes were seen for the specific intra-molecular hydrogen bonding; thus, there was no strong intra-molecular hydrogen bonding between any atoms in the title molecule. The red spikes appear from 0.02 to 0.05 a.u., representing the strong steric repulsion observed between the oxygen of nitrates in NG. The RDG plot shows a weak van der Waals force of attraction between oxygen and hydrogen, which is more prominent than strong intra-molecular hydrogen bonding, with values ranging from −0.02 a.u. to 0.01 a.u. The van der Waals force of attraction between hydrogen and oxygen in the nitrate group is more favorable, as observed from the isosurface, because the atoms are far apart than the ideal distance for hydrogen bonding.

Electrostatic potential (ESP) surface analysis

ESP analysis provides information on the distribution of charges on the surface of the molecule. It allows for the identification of reactive sites based on the location of electrophilic and nucleophilic sites (Chaudhary *et al.*, 2020; Paneru *et al.*, 2024). The most positive potential region is represented by the blue color, and the most negative potential region is represented by the red color. The potential rises in the following order: red < orange < yellow < green < blue (Joshi, 2016). The blue and orange dots on the ESP surface represent the points of minimum and maximum potential, respectively (Fathima Rizwana *et al.*, 2019). The value of ESP shown in Fig. 5 represents the surface extrema of NG. The ESP map shows that oxygen and nitrogen in nitrate are the nucleophiles; they lie in the red color region and have a negative potential. In the blue color region are the electrophilic hydrogen atoms with carbon that have positive potential. The global minimum potential of –15.60 kcal/mol was associated with N11, whereas the maximum potential of 41.31 kcal/mol was associated with H16 of NG. This demonstrates that H16 is the best electrophile and N11 is the best nucleophile, forming the ideal locations for intermolecular bonding for biological interactions and contributing to the formation of crystal packing.

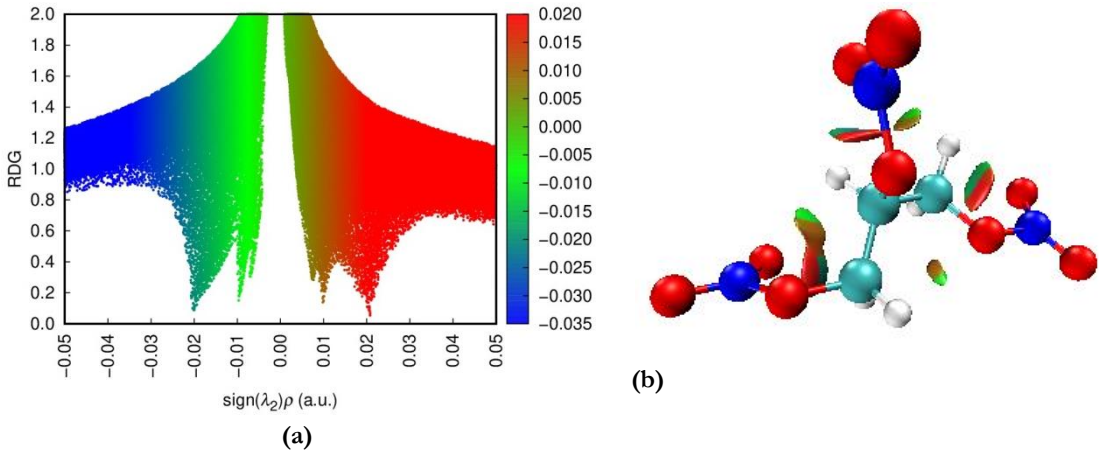

Figure 4. (a) The RDG scatter plot and (b) isosurface showing non-covalent interactions in nitroglycerin.

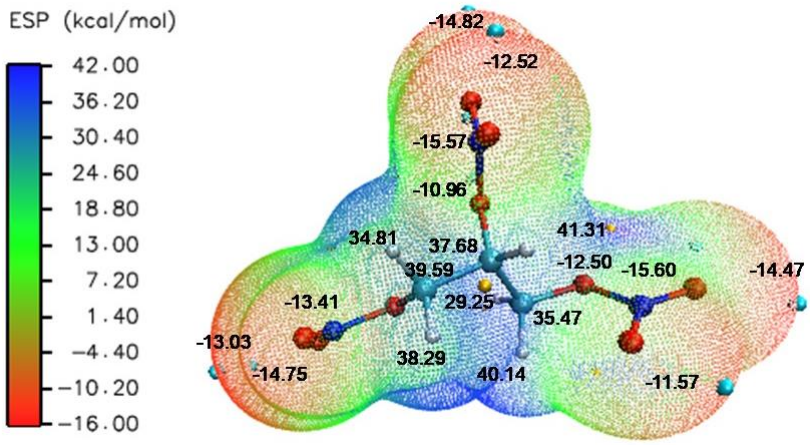

Figure 5. ESP mapped molecular vdW surface of nitroglycerin.

Frontier molecular orbital and density of state

Frontier molecular orbitals, specifically the HOMO and LUMO are crucial for understanding molecular interactions and predicting chemical reactivity and stability (T. Chaudhary *et al.*, 2021). LUMO accepts electrons, and HOMO donates them. The reactivity and stability of the molecule are predicted by the energy gap that exists between HOMO and LUMO (M. K. Chaudhary *et al.*, 2021). The density of states is an effective tool for displaying molecular orbitals and their compositions, as well as revealing how they affect reactivity and electronic structure. The DOS spectrum was generated with a full width at half maximum of 0.3 eV using GaussSum 3.0 software. The HOMO-LUMO plot and the DOS spectrum of NG in ethanol solvent and gaseous medium are depicted in Fig. 6. The energy gap between HOMO and LUMO in the gaseous medium was found to be 6.684 eV, whereas in solvent ethanol it was found to be 6.628 eV, which was the same as the energy gap found in the DOS spectrum. The HOMO-LUMO energy gap for trimetazidine (TMZ), a drug beneficial for heart disease and heart failure with a similar kind of structure, was calculated to be 5.270 eV by using the B3LYP/6-311+G(d,p) level of theory, which indicates that NG is less reactive than the TMZ (Meenakshi *et al.*, 2010). In the DOS spectrum, red lines indicate the LUMO, and green lines indicate the HOMO. Virtual orbitals represent acceptor orbitals, and occupied orbitals represent donor orbitals. The energy gap in solvent ethanol was smaller than in a gaseous medium, indicating that nitroglycerin is more reactive, polarizable in the solvent, and stable in a gaseous medium.

Global reactivity descriptors

When it comes to molecular interactions, from HOMO is an electron donor whose energy is related to ionization potential, and LUMO is an electron acceptor whose energy is associated with electron affinity (Miar *et al.*, 2021). The ionization potential is ($I = -E_{HOMO}$), and the electron affinity is ($A = -E_{LUMO}$). According to the Koopmans theorem, global reactivity descriptors are defined in terms of ionization potential and electron affinity (Koopmans, 1934). The global reactivity descriptors, in terms of the ionization potential (I) and electron affinity (A), are described by the following equations (Parr *et al.*, 1999; Parr & Pearson, 1983).

$$\text{Electronegativity } (\chi) = \frac{1}{2}(\mathrm{I} + \mathrm{A})$$

$$\text{Chemical Potential } (\mu) = -\chi = -\frac{1}{2}(\mathrm{I} + \mathrm{A})$$

$$\text{Global Hardness } (\eta) = \frac{1}{2}(\mathrm{I} - \mathrm{A})$$

$$\text{Softness}(\mathrm{S}) = \frac{1}{2\eta}$$

$$\text{Global Electrophilicity index } (\omega) = \frac{\mu^2}{2\eta}$$

The global reactivity descriptors of NG are presented in Table 3. The ionization potential of NG in solvent ethanol was found to be lower than that in a gaseous medium. In contrast, electron affinity is greater in a gaseous medium, indicating that it is a good electron donor in the solvent and a good acceptor in the gaseous medium. The lower global softness S in a gaseous medium compared to a solvent ethanol indicates that intra-molecular charge transfer is more likely in a solvent, which increases reactivity. The global electrophilicity index (ω), was found to be higher in the gaseous medium, indicating that it is a stronger electrophile than in solvent ethanol.

UV-Vis spectrum and electronic transition

UV-Vis spectroscopy provides a more detailed illustration of electron transitions in molecular orbitals, as well as insight into the various interactions within and between molecules (Sirajuddin *et al.*, 2013). The electronic transition of NG was calculated using TD-DFT in the IEF-PCM model in the gaseous phase and ethanol solvent, and the UV-Vis spectrum was plotted. The UV-Vis spectrum of NG in a gaseous medium and solvent ethanol is shown in Fig. 7. Table 4 displays the main transitions along with their oscillator strength, excitation energy, and absorption wavelengths. The first excited state of NG arises in a gaseous medium when electrons transition from HOMO–2→LUMO, with an absorption wavelength of 257.41 nm. In solvent ethanol,

it occurs when electrons transition from HOMO–2→LUMO+1, with an absorption wavelength of 255.02 nm. Because the polarity of the solvent increases, the absorption in it shifts to a shorter wavelength, resulting in a blue shift (Joshi *et al.*, 2011). Trimetazidinene, a similar type of molecule, had an experimental absorption wavelength of 270.4 nm in n-hexane, which is consistent with our calculation for NG (Meenakshi *et al.*, 2010). Because a solvent allows charge transfer more easily than a gaseous medium, its band gap decreases, which increases its reactivity.

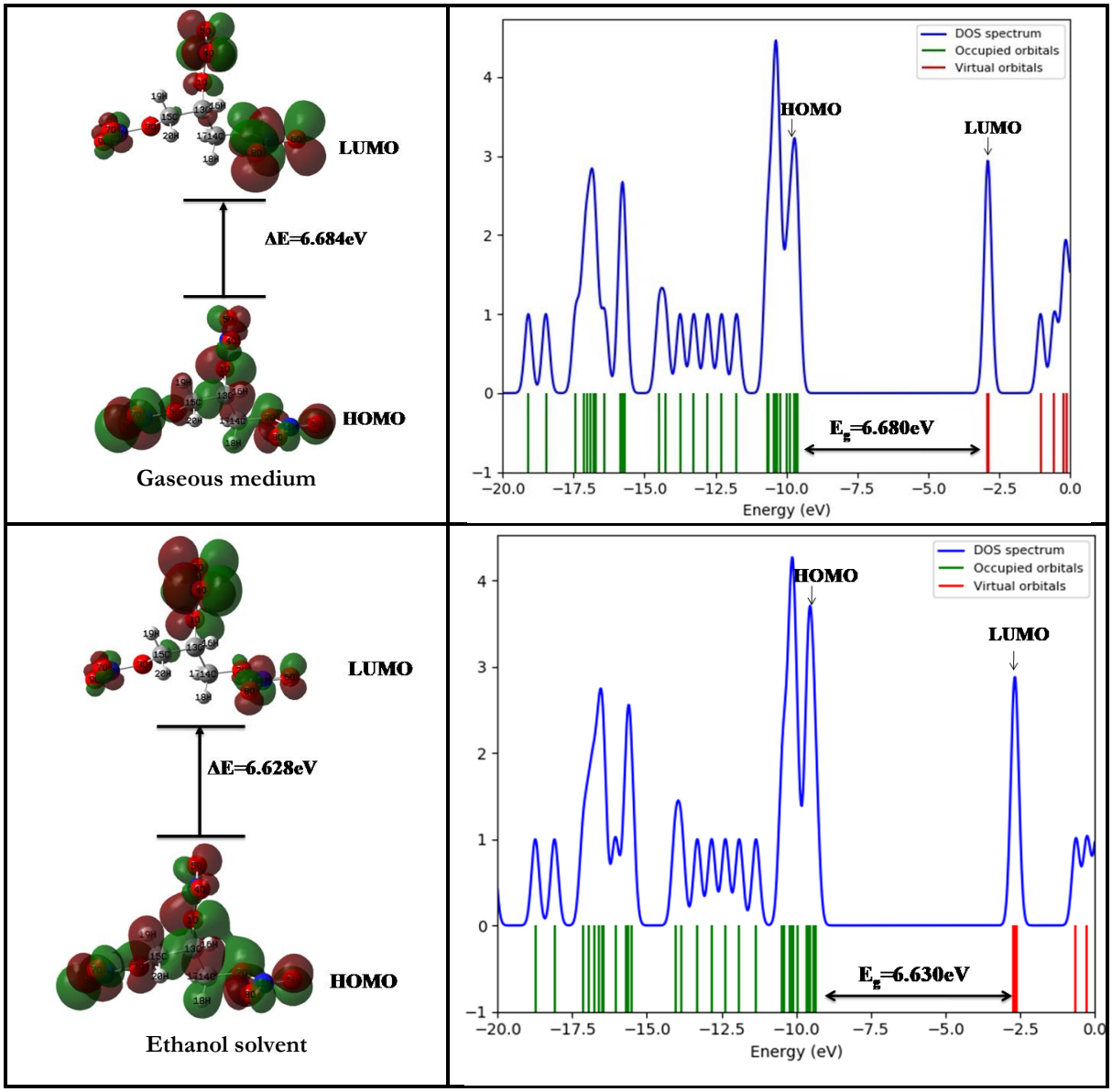

Fig. 6. HOMO–LUMO plots and DOS spectrum for the nitroglycerin in gaseous and solvent ethanol.

Table. 3. Global reactivity descriptors ionization potential (I), electron affinity (A), band gap (I-A), electronegativity (χ), chemical potential (μ), chemical hardness (η), softness (S), and electrophilicity index (ω) of nitroglycerin.

Medium	I(eV)	A(eV)	(I– A)(eV)	χ(eV)	μ(eV)	η(eV)	S(eV^{-1})	ω(eV)	ΔNmax
Gaseous	9.6046	2.9203	6.6843	6.2625	–6.2625	3.3422	0.1496	5.8672	1.8738
Ethanol	9.3352	2.7067	6.6285	6.0210	–6.0210	3.3143	0.1509	5.4691	1.8167

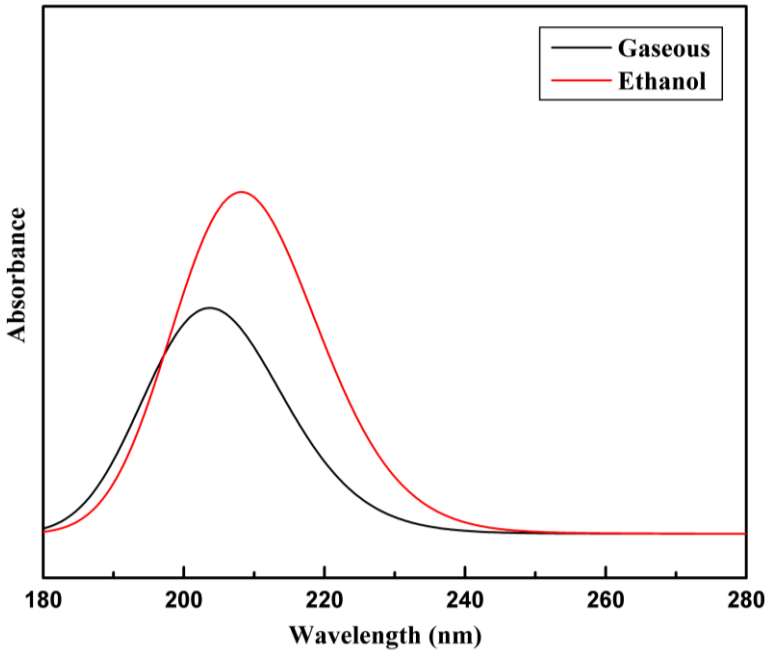

Fig. 7. The UV-Vis absorption spectrum of nitroglycerin in gaseous medium and in solvent.

Table. 4. The parameters of electronic transitions as observed in the UV-Vis spectrum for nitroglycerin, including absorption wavelength, energy gap, excitation energy, and oscillator strength, in both gaseous medium and solvent ethanol.

Medium	Excited state	Excitation energy (eV)	λ_{max}	Oscillator strength (f)	Energy gap (eV)	Major contribution (%)
Gaseous	1	4.82	257.41	0.0001	6.807	HOMO–2→LUMO (52%)
	5	5.66	219.04	0.0017	7.514	HOMO–9→LUMO (52%)
	9	6.16	201.08	0.0020	6.742	HOMO–1→LUMO (48%)
Ethanol	1	4.86	255.02	0.0001	6.853	HOMO–2→LUMO+1(59%)
	5	5.67	218.79	0.0038	7.521	HOMO–9→LUMO+1 (48%)
	7	5.92	209.45	0.0731	6.651	HOMO→LUMO+1(61%)

Natural bond orbital analysis

Natural bond orbital (NBO) investigates the hyperconjugative interactions and delocalization of charge between bonding and antibonding orbitals, which provides insight into stabilizing phenomena (Sebastian & Sundaraganesan, 2010). The stability of a molecular system is known by the strength of interaction, which is determined from the stabilization energy E(2). Stronger donor-acceptor interaction is indicated by a higher stabilization energy value (Weinhold & Landis, 2005). Table 5 displays the stabilization energy for the most stable conformer of the NG, which was determined at the B3LYP/6-311++G(d,p) level of theory. Oxygens O2, O3, O4, O5, O6, O7, O8, and O9 donate the lone pair of electrons, and they were accepted by N10, N11, and N12. The interactions π(O4-N10)→σ*(O5-N10), σ(O5-N10)→π*(O4-N10), LP(3)O8→σ*(O6-N11), and LP(3)O9→π*(O7-N12) have higher stabilization energies of 277.41, 278.89, 181.47, and 137.42 kcal/mol, respectively. These interactions are crucial for the stabilization of NG.

Mulliken charge analysis

Mulliken atomic charges contribute to understanding the electronic structure and behavior of chemical systems by providing information on their dipole moment, electronic distribution, and polarizability (Mulliken, 1955). The calculated atomic charges for each atom of NG with the B3LYP/6-311++G(d,p) level of theory are shown in Fig. 8. The Mullikens charges on each atom of NG are presented in Table 6. All oxygen atoms and hydrogen atoms were clearly shown to have positive charges, while all carbon and nitrogen atoms had negative charges. The negative charges were found in N10, N11, N12, C13, C14, and C15, whereas positive charges were found in O1, O2, O3, O4, O5, O6, O7, O8, O9, H16, H17, H18, H19, and H20. The highest positive and negative charges were found in atoms H16 and C14, respectively.

Table 5. NBO basis of conformer I of nitroglycerin by the analysis of second-order perturbation theory analysis of Fock matrix.

Donor NBO(i)	ED (i)/e	AcceptorNBO(j)	ED(j)/e	C E(2)[a] kcal/mol	Col E(j)-E(i)[b] u	C F(i,j)[c]a.u
σ(O4-N10)	1.894	σ*(O5-N10)	0.344	93.60	1.66	0.375
π(O4-N10)	1.739	σ*(O5-N10)	0.344	277.41	1.13	0.511
σ(O5-N10)	1.712	π*(O4-N10)	0.324	278.89	0.92	0.456
σ(O5-N10)	1.712	σ*(O4-N10)	0.147	70.76	0.70	0.207
LP(2)O2	1.851	σ*(O6-N11)	0.610	27.57	0.20	0.076
LP(2)O3	1.857	π*(O7-N12)	0.612	22.80	0.24	0.075
LP(2)O4	1.832	σ*(O1-N10)	0.253	36.52	0.39	0.109
LP(2)O4	1.832	π*(O5-N10)	0.047	14.13	0.79	0.097
LP(2)O5	1.825	σ*(O1-N10)	0.253	36.67	0.38	0.107
LP(2)O5	1.825	σ*(O4-N10)	0.147	13.15	0.78	0.091
LP(2)O6	1.827	σ*(O2-N11)	0.249	35.78	0.38	0.106
LP(2)O6	1.827	σ*(O8-N11)	0.103	16.88	0.71	0.100
LP(2)O7	1.832	σ*(O3-N12)	0.251	36.90	0.39	0.109
LP(2)O7	1.832	σ*(O9-N12)	0.047	14.36	0.78	0.098
LP(2)O8	1.835	σ*(O2-N11)	0.249	35.57	0.39	0.108
LP(2)O8	1.835	π*(O6-N11)	0.046	14.18	0.79	0.097
LP(3)O8	1.462	σ*(O6-N11)	0.610	181.47	0.16	0.157
LP(3)O8	1.462	σ*(O8-N11)	0.103	24.83	0.71	0.134
LP(2)O9	1.827	σ*(O3-N12)	0.251	36.34	0.38	0.107
LP(2)O9	1.827	σ*(O7-N12)	0.101	15.93	0.71	0.096
LP(3)O9	1.452	π*(O7-N12)	0.613	137.42	0.18	0.143

[a]E(2) is the stabilization energy represented by hyper conjugative interaction .
[b]Energy difference between donor (i) and acceptor (j) NBO orbitals.
[c]F(i,j) is the element of the Fock matrix between NBO orbitals i and j.

Thermodynamic properties

The study of thermodynamic properties such as enthalpy, specific heat capacity, and entropy can be used to investigate the effect of temperature on chemical reactions, as well as to assess the stability and chemical reactivity of chemical species (Chaudhary *et al.*, 2022; Joshi *et al.*, 2014). The thermal behaviour of NG studied by Nakahama *et. al.* reported the thermal decomposition of NG was at 453 K (Nakahama *et al.*, 2007). Above 140 °C, NG undergoes first-order thermal breakdown in the vapor phase; however, in the liquid phase, the decomposition is nearly first-order and autocatalytic below 140 °C (Waring & Krastins, 1970). In this study, the thermodynamical parameters enthalpy(H_m^0), specific heat capacity at constant pressure ($C_{p,m}^0$), and entropy(S_m^0) for the most stable conformer of NG calculated at the B3LYP/6-311++G(d,p) level of theory between a temperature range of (50−350)K. The total energy, zero-point energy, specific heat, and entropy of NG at room temperature are calculated to be −958.467 a.u, 326.166 J/mol, 201.970 J/K, and 541.984 $Jmol^{-1}K^{-1}$, respectively. These values are in good agreement with the corresponding values −958.166 a.u, 319.680, 213.710 J/K, and 533.870 $Jmol^{-1}K^{-1}$, respectively, calculated at the B3LYP/6-31*G level of theory (Gong & Xiao, 2001). The enthalpy, specific heat capacity and entropy of the NG were calculated from (50-350)K and the variation of stated thermodynamic parameters with the variation of temperature was plotted with the polynomial fit, which is given in Fig. 9. In the graph, the values of R^2 for enthalpy, specific heat capacity, and entropy were found to be 0.9999, 0.9996, and 0.9983, respectively, indicating that these thermodynamical parameters increase with increasing temperature because the molecule's vibrational energy increases with rise in temperature (T. Chaudhary & Joshi, 2022). The correlation equations for enthalpy, specific heat capacity, and entropy are as follows:

$$H_m^0 = 77.8432 + 0.0136T - 0.5781T^2 \ (R^2 = 0.9999)$$
$$C_{p,m}^0 = 13.0274 + 0.1206T - 0.0094T^2 (R^2 = 0.9996)$$
$$S_m^0 = 56.9180 + 0.0136T + 0.0578T^2 \ (R^2 = 0.9983)$$

These equations provide a route for interaction with another molecule and help in the estimation of the direction of chemical reactions as well as the prediction of the Gibbs free energy and spontaneity of the reaction.

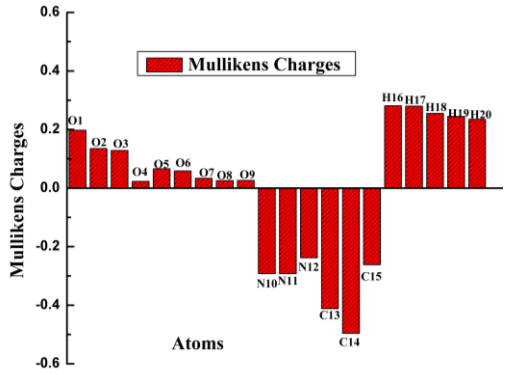

Figure 8. Distribution of Mulliken charges on the molecule nitroglycerin.

Table 6. Mullikens charges on each atom of nitroglycerin.

Atoms	Charges	Atoms	Charges
O1	0.1977	N11	–0.2921
O2	0.1353	N12	–0.2381
O3	0.1286	C13	–0.4117
O4	0.0231	C14	–0.4959
O5	0.0661	C15	–0.2615
O6	0.0589	H16	0.2813
O7	0.0337	H17	0.2799
O8	0.0256	H18	0.2554
O9	0.0262	H19	0.2448
N10	–0.2922	H20	0.2349

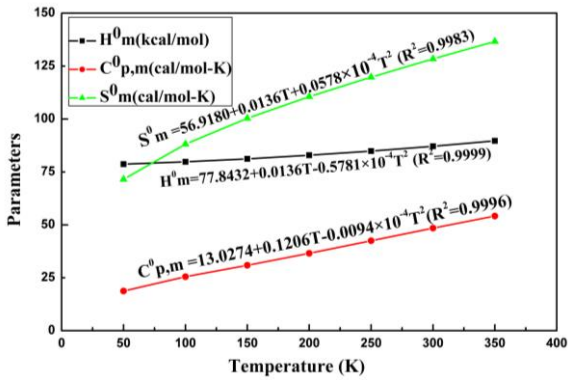

Figure 9. Correlation graph of enthalpy (H^o_m), specific heat ($C^o_{m,p}$) and entropy (S^o_m) of nitroglycerin with temperature.

CONCLUSIONS

This work presents the study of molecular structure with conformational analysis of nitroglycerin by a quantum chemical approach. Ten conformers of nitroglycerin were obtained; five of them have an energy difference of less than 0.56 kcal/mol compared to the lowest energy conformer. Conformer I of nitroglycerin was the most stable, with a minimum ground state energy of –601447.0664 kcal/mol. This conformer was used in further studies of NG. The optimized structure parameters, such as bond length and bond angles, were found to match the experimental values. Non-covalent interaction revealed that there was no intra-molecular hydrogen bonding, but there was steric repulsion between the oxygen of the nitrate group. The minimum potential of –15.60 kcal/mol was attributed to N11, and the maximum potential of 41.31 kcal/mol was associated with H16. It was found that the energy gap in the DOS spectrum in gaseous medium and ethanol was the same as the HOMO-LUMO gap. The global softness in solvent ethanol was greater than in the gaseous medium, which indicates that the title molecule is more reactive and polarizable in solvent. The absorption wavelength in the gaseous medium was found to be 257.41 nm, and in solvent it decreases to 255.02 nm, resulting in a blue shift that allows the transfer of charge more easily. Higher stabilization energy for the conjugative interaction from donor to acceptor stabilizes the molecule. Mulliken charge analysis predicted that the highest positive and negative charge was contained in N12 and O3, respectively. Moreover, the thermodynamical parameters were found to be highly correlated with the rise in temperature.

ACKNOWLEDGMENTS

T.R. Paneru acknowledges DST, India, for granting partial fellowship (INSA/DST-ISRF/2023/NEP/15/13. He also acknowledges the Far Western University, Mahendranagar, Kanchanpur, Nepal

AUTHOR CONTRIBUTIONS

T.R. Paneru: writing-original draft, investigation, and data analysis; P. Tandon: software facility and supervision; B.D. Joshi: reviewing, analysis, and supervision.

CONFLICT OF INTEREST

There are no conflicts to interests.

DATA AVAILABILITY STATEMENT

The data that support the findings of this study are available from the corresponding author, upon reasonable request.

REFERENCES

Antipin, M.Y., Struchkov, Y.T., Philippov, V.A., Tsirel'Son, V.G., Ozerov, R.P., & Svetlov, B.S. (1984). Structure of 1,2,3-propanetriol trinitrate (β Modification), $C_3H_5N_3O_9$. *Acta crystallography, C40,* 2096-2098

Becke, A.D. (1993). Density-functional thermochemistry. III. The role of exact exchange. *The Journal of Chemical Physics*, *98*(7), 7. https://doi.org/10.1063/1.464913

Chaudhary, M.K., Karthick, T., Joshi, B.D., Prajapati, P., De Santana, M.S.A., Ayala, A.P., Reeda, V.S.J., & Tandon, P. (2021). Molecular structure and quantum descriptors of cefradine by using vibrational spectroscopy (IR and Raman), NBO, AIM, chemical reactivity and molecular docking. *Spectrochimica Acta*

Part A: Molecular and Biomolecular Spectroscopy, *246*, 118976. https://doi.org/10.1016/j.saa.2020.118976

Chaudhary, M.K., Prajapati, P., & Joshi, B.D. (2020). Quantum chemical calculation and DFT study of sitagliptin: Insight from computational evaluation and docking approach. *Journal of Nepal Physical Society*, *6*(1), 73–83. https://doi.org/10.3126/jnphyssoc.v6i1.30553

Chaudhary, M.K., Srivastava, A., Singh, K.K., Tandon, P., & Joshi, B.D. (2020). Computational evaluation on molecular stability, reactivity, and drug potential of frovatriptan from DFT and molecular docking approach. *Computational and Theoretical Chemistry*, *1191*, 113031. https://doi.org/10.1016/j.comptc.2020.113031

Chaudhary, T., Chaudhary, M.K., & Joshi, B.D. (2021). Topological and reactivity descriptor of carisoprodol from DFT and molecular docking approach. *Journal of Institute of Science and Technology*, *26*(1), 74–82. https://doi.org/10.3126/jist.v26i1.37828

Chaudhary, T., Chaudhary, M.K., & Joshi, B.D. (2022). A Theoretical study on charge transfer and hyperpolarizability of (S)-2-amino-3-(3,4-dihydroxyphenyl)-2-methyl-propanoic acid. *Journal of Nepal Physical Society*, *8*(1), 16–21. https://doi.org/10.3126/jnphyssoc.v8i1.48280

Chaudhary, T., & Joshi, B.D. (2022). Electronic, thermodynamic properties, nonlinear optical responses, and molecular docking studies on dephalexin. *Journal of Institute of Science and Technology*, *27*(1), 83–92. https://doi.org/10.3126/jist.v27i1.46361

Chen, Z., Zhang, J., & Stamler, J.S. (2002). Identification of the enzymatic mechanism of nitroglycerin bioactivation. *Proceedings of the National Academy of Sciences*, *99*(12), 8306–8311. https://doi.org/10.1073/pnas.122225199

Cossi, M., Scalmani, G., Rega, N., & Barone, V. (2002). New developments in the polarizable continuum model for quantum mechanical and classical calculations on molecules in solution. *The Journal of Chemical Physics*, *117*(1), 43–54. https://doi.org/10.1063/1.1480445

Dennington, R., Keith, T.A., Millam, John, M., (2016) GaussView 06 *Semichem Inc.* Shawnee Mission, KS .

Dunning, T.H. (1989). Gaussian basis sets for use in correlated molecular calculations. I. The atoms boron through neon and hydrogen. *The Journal of Chemical Physics*, *90*(2), 2. https://doi.org/10.1063/1.456153

Fathima Rizwana, B., Prasana, J.C., Muthu, S., & Abraham, C.S. (2019). Molecular docking studies, charge transfer excitation and wave function analyses (ESP, ELF, LOL) on valacyclovir: A potential antiviral drug. *Computational Biology and Chemistry*, *78*, 9–17. https://doi.org/10.1016/j.compbiolchem.2018.11.014

Ferreira, J.C.B., & Mochly-Rosen, D. (2012). Nitroglycerin use in myocardial infarction patients risks and benefits. *Circulation Journal*, *76*(1), 15–21. https://doi.org/10.1253/circj.CJ-11-1133

Frisch, M.J., Trucks, G.W., Schlegel, H.B., Scuseria, G.E., Robb, M.A., Cheeseman, J.R., Scalmani, G., Barone, V., Mennucci, B., Petersson, G.A., Nakatsuji, H., Caricato, M., Li, X., Hratchian, H.P., Izmaylov, A.F., Bloino, J., Zheng, G., Sonnenberg, J.L., Hada, M., & Fox, D.J. (2016). *Gaussian 16 Revision*.

Glendening, E.D., Reed, A.E., Carpenter, J.E., & Weinhold, F. (2003). NBO 3.1 *Gaussian Inc.*, Pittsburg.

Gong, X.D., & Xiao, H.M. (2001). Studies on the molecular structures, vibrational spectra and thermodynamic properties of organic nitrates using density functional theory and ab initio methods. *Journal of Molecular Structure: THEOCHEM*, *572*(1–3), 213–221. https://doi.org/10.1016/S0166-1280(01)00633-9

Hohenberg, P., & Kohn, W. (1964). Inhomogeneous electron gas. *Physical Review*, *136*(3B), B864-B871. https://doi.org/10.1103/PhysRev.136.B864.

Humphrey, W., Dalke, A., & Schulten, K. (1996). VMD: Visual molecular dynamics. *Journal of Molecular Graphics*, *14*(1), 1. https://doi.org/10.1016/0263-7855(96)00018-5

Jia, Z., Pang, H., Li, H., & Wang, X. (2019). A density functional theory study on complexation processes and intermolecular interactions of triptycene-derived oxacalixarenes. *Theoretical Chemistry Accounts*, *138*(9), 113. https://doi.org/10.1007/s00214-019-2502-6

Johnson, E.R., Keinan, S., Mori-Sánchez, P., Contreras-García, J., Cohen, A.J., & Yang, W. (2010). Revealing Noncovalent Interactions. *Journal of the American Chemical Society*, *132*(18), 18. https://doi.org/10.1021/ja100936w

Joshi, B.D. (2016). Chemical reactivity, dipole moment and first hyperpolarizability of aristolochic acid I. *Journal of Institute of Science and Technology*, *21*(1), 1–9. https://doi.org/10.3126/jist.v21i1.16030

Joshi, B.D., Mishra, R., Tandon, P., Oliveira, A.C., & Ayala, A.P. (2014). Quantum chemical studies of structural, vibrational, NBO and hyperpolarizability of ondansetron hydrochloride. *Journal of Molecular Structure*, *1058*, 31–40. https://doi.org/10.1016/j.molstruc.2013.10.062

Joshi, B.D., Srivastava, A., Tandon, P., & Jain, S. (2011). Molecular structure, vibrational spectra and HOMO, LUMO analysis of yohimbine hydrochloride by density functional theory and ab initio Hartree–Fock calculations. *Spectrochimica Acta Part A: Molecular and Biomolecular Spectroscopy*, *82*(1), 1. https://doi.org/10.1016/j.saa.2011.07.047

Koopmans, T. (1934). Über die zuordnung von wellenfunktionen und eigenwerten zu den einzelnen elektronen eines atoms. *Physica*, *1*(1–6), 104-113. https://doi.org/10.1016/S0031-8914(34)90011-2

Lu, T., & Chen, F. (2012). Multiwfn: A multifunctional wavefunction analyzer. *Journal of Computational Chemistry*, *33*(5), 5. https://doi.org/10.1002/jcc.22885

Marsh, N., & Marsh, A. (2000). A short history of nitroglycerin and nitric oxide in pharmacology and physiology. *Clinical and Experimental Pharmacology and*

Physiology, *27*(4), 313–319. https://doi.org/10.1046/j.1440-1681.2000.03240.x

Meenakshi, R., Jaganathan, L., Gunasekaran, S., & Srinivasan, S. (2012). Molecular structure and vibrational spectroscopic investigation of nitroglycerin using DFT calculations. *Molecular Simulation*, *38*(3), 204–210. https://doi.org/10.1080/08927022.2011.614240

Meenakshi, R., Jagannathan, L., Gunasekaran, S., & Srinivasan, S. (2010). FT-IR, FT-Raman and UV-Vis spectra and quantum chemical investigation of trimetazidine. *Molecular Simulation*, *36*(12), 969–977. https://doi.org/10.1080/08927022.2010.497925

Miar, M., Shiroudi, A., Pourshamsian, K., Oliaey, A.R., & Hatamjafari, F. (2021). Theoretical investigations on the HOMO–LUMO gap and global reactivity descriptor studies, natural bond orbital, and nucleus-independent chemical shifts analyses of 3-phenylbenzo]thiazole-2(3 H)-imine and its para -substituted derivatives: Solvent and substituent effects. *Journal of Chemical Research*, *45*(1–2), 1–2. https://doi.org/10.1177/1747519820932091

Moazemi, K., Chana, J.S., Willard, A.M., & Kocheril, A.G. (2003). Intravenous vasodilator therapy in congestive heart failure: *Drugs & Aging*, *20*(7), 485–508. https://doi.org/10.2165/00002512-200320070-00002

Mulliken, R.S. (1955). Electronic population analysis on LCAO–MO molecular wave functions I. *The Journal of Chemical Physics*, *23*(10), 1833–1840. https://doi.org/10.1063/1.1740588

Nakahama, M., Katoh, K., Kawaguchi, S., Kubota, S., Wada, Y., Ogata, Y., & Arai, M. (2007). Study on the thermal behavior of nitroglycerine. *Science and Technology of Energetic Materials*, 68(1), 21-24.

O'boyle, N.M., Tenderholt, A.L., & Langner, K.M. (2008). cclib: A library for package-independent computational chemistry algorithms. *Journal of Computational Chemistry*, *29*(5), 839–845. https://doi.org/10.1002/jcc.20823

Paneru, T.R., Chaudhary, M.K., Tandon, P., & Joshi, B.D. (2024). Cocrystal screening of benznidazole based on electronic transition, molecular reactivity, hydrogen bonding, and stability.*Journal of molecular modeling,* https://doi.org/10.1007/s00894-024-06146-1

Paneru, T.R., Chaudhary, M.K., Tandon, P., Chaudhary, T., & Joshi, B.D. (2024). Theoretical study on molecular stability, reactivity, and drug potential of cirsilineol from DFT and molecular docking methods. *Chemical Physics Impact*, *8*, 100641. https://doi.org/10.1016/j.chphi.2024.100641

Parr, R.G., & Pearson, R.G. (1983). Absolute hardness: Companion parameter to absolute electronegativity. *Journal of the American Chemical Society*, *105*(26), 7512-7516. https://doi.org/10.1021/ja00364a005.

Parr, R.G., Szentpály, L.V., & Liu, S. (1999). Electrophilicity Index. *Journal of the American Chemical Society*, *121*(9), 9. https://doi.org/10.1021/ja983494x

Pei, L., Dong, K., Tang, Y., Zhang, B., Yu, C., & Li, W. (2017). A density functional theory study of the decomposition mechanism of nitroglycerin. *Journal of Molecular Modeling*, *23*(9), 269. https://doi.org/10.1007/s00894-017-3440-7

Sebastian, S., & Sundaraganesan, N. (2010). The spectroscopic (FT-IR, FT-IR gas phase, FT-Raman and UV) and NBO analysis of 4-Hydroxypiperidine by density functional method. *Spectrochimica Acta Part A: Molecular and Biomolecular Spectroscopy*, *75*(3), 3. https://doi.org/10.1016/j.saa.2009.11.030

Sidhu, M., Boden, W.E., Padala, S.K., Cabral, K., & Buschmann, I. (2015). Role of short-acting nitroglycerin in the management of ischemic heart disease. *Drug Design, Development and Therapy*, 4793. https://doi.org/10.2147/DDDT.S79116

Sirajuddin, M., Ali, S., & Badshah, A. (2013). Drug–DNA interactions and their study by UV-Visible, fluorescence spectroscopies and cyclic voltametry. *Journal of Photochemistry and Photobiology B: Biology*, *124*, 1–19. https://doi.org/10.1016/j.jphotobiol.2013.03.013

Stratmann, R.E., Scuseria, G.E., & Frisch, M.J. (1998). An efficient implementation of time-dependent density-functional theory for the calculation of excitation energies of large molecules. *The Journal of Chemical Physics*, *109*(19), 8218–8224. https://doi.org/10.1063/1.477483

Waring, C.E., & Krastins, G. (1970). Kinetics and mechanism of the thermal decomposition of nitroglycerin. *The Journal of Physical Chemistry*, *74*(5), 999–1006. https://doi.org/10.1021/j100700a007

Weinhold, F., & Landis, C.R. (2005). *Valency and Bonding: A Natural Bond Orbital Donor-Acceptor Perspective*. Cambridge University Press.

Yan, Q., Zhu, W., Pang, A., Chi, X., Du, X., & Xiao, H. (2013). Theoretical studies on the unimolecular decomposition of nitroglycerin. *Journal of Molecular Modeling*, *19*(4), 1617–1626. https://doi.org/10.1007/s00894-012-1724-5